

基于 Hamilton 体系的功能梯度矩形板 自由振动问题的解析解*

张继超¹, 钟心雨², 陈一鸣¹, 石越卿¹, 郭程洁¹, 李锐¹

(1. 大连理工大学 力学与航空航天学院

工业装备结构分析优化与 CAE 软件全国重点实验室, 辽宁 大连 116024;

2. 西安交通大学 航天航空学院 多尺度力学-医学交叉实验室, 西安 710049)

(本刊编委李锐来稿)

摘要: 对于功能梯度矩形板的自由振动问题, 寻求既满足高阶偏微分控制方程又满足各种非 Lévy 型边界条件的振型函数十分困难, 这使得利用传统方法难以解析求解该类问题. 该文拓展了近年来发展的基于 Hamilton 体系的辛叠加方法, 将其成功应用于功能梯度矩形板自由振动问题的解析求解. 求解方案将原问题拆分成子问题, 并引入物理中性面消除了由于横向材料不均匀产生的拉弯耦合效应, 采用在传统 Lagrange 体系中无法使用的分离变量、辛本征展开等数学方法对子问题进行求解, 最后通过叠加获得了原问题的解答. 辛叠加方法的优点是不需要事先假定解的形式, 克服了传统半逆解法的限制, 能够获得更多复杂问题的解析解. 将该方法的求解结果与数值解进行对比, 证明了其正确性, 并在此基础上进行了定量的参数分析, 研究了不同边界条件、材料分布和长宽比对板固有频率的影响.

关键词: 功能梯度板; 自由振动; Hamilton 体系; 解析解

中图分类号: O302 **文献标志码:** A **DOI:** 10.21656/1000-0887.440279

Hamiltonian System-Based Analytical Solutions to Free Vibration Problems of Functionally Graded Rectangular Plates

ZHANG Jichao¹, ZHONG Xinyu², CHEN Yiming¹,
SHI Yueqing¹, GUO Chengjie¹, LI Rui¹

(1. *State Key Laboratory of Structural Analysis, Optimization and CAE Software for Industrial Equipment,
School of Mechanics and Aerospace Engineering,
Dalian University of Technology, Dalian, Liaoning 116024, P.R.China;*

* 收稿日期: 2023-09-20; 修订日期: 2023-11-05

基金项目: 国家自然科学基金(12372067; 12022209; 11972103)

作者简介: 张继超(1997—), 男, 硕士生(E-mail: 690484356@mail.dlut.edu.cn);

钟心雨(1999—), 女, 硕士生(E-mail: zhongxinyu@stu.xjtu.edu.cn);

陈一鸣(1999—), 男, 硕士生(E-mail: YimingChen@mail.dlut.edu.cn);

石越卿(1995—), 男, 博士生(E-mail: shiyueqing@mail.dlut.edu.cn);

郭程洁(1997—), 女, 博士生(E-mail: 1784971935@mail.dlut.edu.cn);

李锐(1985—), 男, 教授, 博士, 博士生导师(通讯作者. E-mail: rui.li@dlut.edu.cn).

引用格式: 张继超, 钟心雨, 陈一鸣, 石越卿, 郭程洁, 李锐. 基于 Hamilton 体系的功能梯度矩形板自由振动问题的解析解[J]. 应用数学和力学, 2024, 45(9): 1157-1171.

2. *Laboratory for Multiscale Mechanics and Medical Science, School of Aerospace Engineering,*

Xi'an Jiaotong University, Xi'an 710049, P.R.China)

(Contributed by LI Rui, M.AMM Editorial Board)

Abstract: Finding vibration mode functions satisfying both high-order partial differential governing equations and various non-Lévy-type boundary conditions is extremely challenging for the free vibration problems of functionally graded rectangular plates, making it difficult to analytically solve the problem with traditional methods. Herein, the newly developed Hamiltonian system-based symplectic superposition method was extended and successfully applied to analytical solutions to the free vibration problems of functionally graded rectangular plates. For the solution methodology, the original vibration problem was divided into sub-problems and the physical neutral plane was introduced to eliminate the stretching-bending coupling effect caused by the transversely non-uniform materials. The sub-problems were analytically solved with some mathematical techniques, i.e., the variable separation and the symplectic eigenvector expansion, which are not applicable in the traditional Lagrangian system. The final solution to an original vibration problem was obtained through the superposition of sub-problems. The symplectic superposition method has the advantage of not requiring the pre-defined solution forms, which overcomes the limitations of traditional semi-inverse methods and allows for obtaining analytical solutions to more complex problems. Comparison of the obtained solutions with the numerical solutions proves the accuracy of the presented method. On this basis, quantitative parameter analyses on the natural frequencies were conducted to reveal the effects of boundary conditions, material distributions and aspect ratios.

Key words: functionally graded plate; free vibration; Hamiltonian system; analytical solution

0 引 言

随着材料科学和制造业的进步,由金属和陶瓷两种材料构成、沿厚度分布平稳变化的功能梯度材料得到了快速发展^[1].功能梯度材料相较于单一的金属或陶瓷材料具有更高的比强度和比刚度,已被广泛应用于航空航天工程、声学工程、土木工程和海洋工程等各个领域^[2].板作为工程中常见的承力结构,其动力问题一直是结构设计时需要重点考虑的问题,因此,功能梯度板自由振动行为的研究引起了科研人员和工程师们的极大关注.

求解板自由振动问题的方法主要分为数值方法和解析方法,其中常见的数值方法包括有限元法^[3-6]、边界元法^[7-8]、无网格法^[9-10]、Ritz法^[11-15]、微分求积法^[16-18]、动刚度法^[19]、有限差分法^[20-21]、等几何法^[22]等.上述数值方法已部分应用于求解功能梯度板的自由振动问题;如 Kumar 等^[23]使用动刚度法求解了功能梯度板的自由振动问题;Yin 等^[24]通过等几何分析研究了功能梯度板的静态弯曲、屈曲和自由振动行为.

由于解析方法在结构快速分析及初步优化设计等方面具有数值方法不能比拟的效率优势,因此即便在数值方法蓬勃发展的今天,解析方法仍然具有不可替代性.然而,在传统求解框架下,高阶偏微分方程的复杂边值问题很难解析求解,这大大限制了解析方法的发展.事实上,除了传统的 Navier 型边界^[25-28]和 Lévy 型边界^[29-31]功能梯度矩形板,其他边界下板自由振动问题的解析解研究较为少见,这与实际工程中对边简支矩形板应用很少的现实相矛盾.因此,寻求一种高效高精度且适用于多种边界条件的解析方法,无论对理论研究还是工程实际都具有重要价值.

本文基于 Hamilton 体系研究功能梯度矩形板的自由振动问题,首先通过引入物理中性面消除了由于功能梯度材料横向不均匀性产生的拉弯耦合效应,随后将功能梯度矩形板自由振动的基本方程导入到 Hamilton 体系当中,通过在辛空间下求解功能梯度矩形板自由振动的 Hamilton 对偶方程,得到了 Lévy 型板的解析解.对于非 Lévy 型板问题,采用辛叠加方法^[32-37]进行求解,先将原问题拆分成子问题,通过上述辛方法分别求解这些子问题而后叠加,便可得到原问题的解答.本文求解了典型非 Lévy 型功能梯度矩形板自由振动问题的解析解,并通过数值解与所得解析解的对比验证了本文方法的正确性.

1 Hamilton 体系的导入

1.1 功能梯度材料

如图 1 所示的功能梯度板,其上层为陶瓷材料、下层为金属材料,沿着板厚度方向材料的分布满足^[23]

$$P(z) = P_m + (P_c - P_m) \left(\frac{1}{2} + \frac{z}{h} \right)^k, \quad -\frac{h}{2} \leq z \leq \frac{h}{2}, \quad (1)$$

式中, P 为材料属性, P_c 和 P_m 分别代表陶瓷材料和金属材料的属性, k 为材料的体积分数指数. 材料属性沿板厚度方向的变化趋势如图 2 所示. 当 k 趋于 0 时, 整块板的材料属性趋于陶瓷材料, 当 k 趋于无穷大时, 趋于金属材料.

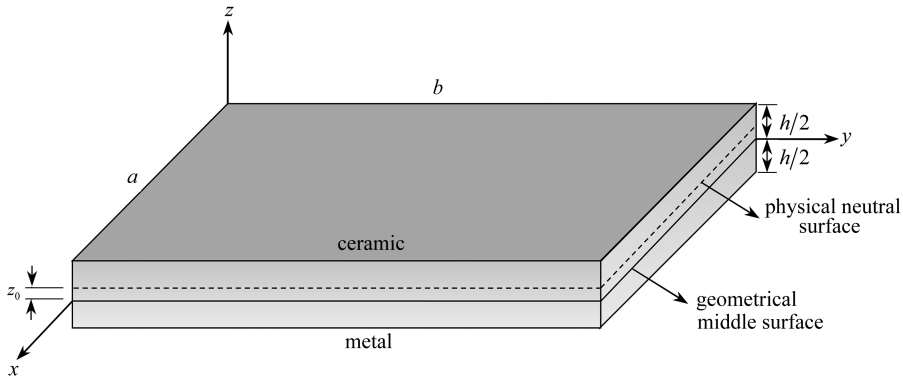


图 1 功能梯度板示意图

Fig. 1 Schematic diagram of a functionally graded plate

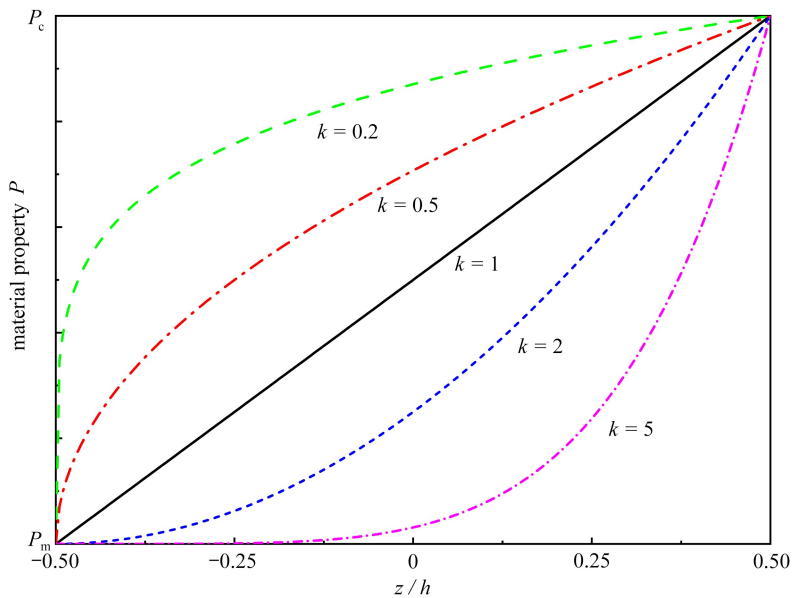


图 2 材料属性沿板厚度方向变化图

Fig. 2 Variations of material properties along the direction of the plate thickness

注 为了解释图中的颜色, 读者可以参考本文的电子网页版本, 后同.

由于横向材料的不均匀性, 本文引入物理中性面的概念, 该中性面由下式确定^[38]:

$$z_0 = \frac{\int_{-h/2}^{h/2} zE(z) dz}{\int_{-h/2}^{h/2} E(z) dz} = \frac{(E_c - E_m)hk}{2(2+k)(E_c + E_mk)}, \quad (2)$$

其中 E 为材料的弹性模量, z_0 为物理中性面到几何中性面的距离.

1.2 基于物理中性面的功能梯度板自由振动的控制方程

当引入物理中性面后,基于经典薄板理论的功能梯度板自由振动的方程会有所改变,下面进行控制方程的重新推导.如图1所示的功能梯度板,其位移表达式为

$$\begin{cases} u(x, y, z) = -(z - z_0) \frac{\partial w}{\partial x}, \\ v(x, y, z) = -(z - z_0) \frac{\partial w}{\partial y}, \\ w(x, y, z) = w(x, y). \end{cases} \quad (3)$$

则功能梯度板的几何方程为

$$\begin{cases} \varepsilon_x = -(z - z_0) \frac{\partial^2 w}{\partial x^2}, \\ \varepsilon_y = -(z - z_0) \frac{\partial^2 w}{\partial y^2}, \\ \gamma_{xy} = -2(z - z_0) \frac{\partial^2 w}{\partial x \partial y}. \end{cases} \quad (4)$$

应力与应变的关系为

$$\begin{Bmatrix} \sigma_x \\ \sigma_y \\ \tau_{xy} \end{Bmatrix} = \frac{E(z)}{1 - \nu^2} \begin{bmatrix} 1 & \nu & 0 \\ \nu & 1 & 0 \\ 0 & 0 & \frac{1 - \nu}{2} \end{bmatrix} \begin{Bmatrix} \varepsilon_x \\ \varepsilon_y \\ \gamma_{xy} \end{Bmatrix}, \quad \begin{Bmatrix} \tau_{yz} \\ \tau_{xz} \end{Bmatrix} = \frac{E(z)}{2(1 + \nu)} \begin{bmatrix} 1 & 0 \\ 0 & 1 \end{bmatrix} \begin{Bmatrix} \gamma_{yz} \\ \gamma_{xz} \end{Bmatrix}. \quad (5)$$

功能梯度板自由振动的控制方程为

$$\begin{cases} \frac{\partial M_x}{\partial x} + \frac{\partial M_{xy}}{\partial y} - Q_x = 0, \\ \frac{\partial M_y}{\partial y} + \frac{\partial M_{xy}}{\partial x} - Q_y = 0, \\ \frac{\partial Q_x}{\partial x} + \frac{\partial Q_y}{\partial y} + \overline{\rho h} \omega^2 w = 0. \end{cases} \quad (6)$$

内力分别为

$$\begin{cases} M_x = \int_{-h/2}^{h/2} \sigma_x (z - z_0) dz = -\bar{D} \left(\frac{\partial^2 w}{\partial x^2} + \nu \frac{\partial^2 w}{\partial y^2} \right), \\ M_y = \int_{-h/2}^{h/2} \sigma_y (z - z_0) dz = -\bar{D} \left(\frac{\partial^2 w}{\partial y^2} + \nu \frac{\partial^2 w}{\partial x^2} \right), \\ M_{xy} = \int_{-h/2}^{h/2} \tau_{xy} (z - z_0) dz = -\bar{D} (1 - \nu) \frac{\partial^2 w}{\partial x \partial y}, \end{cases} \quad (7)$$

$$Q_x = \int_{-h/2}^{h/2} \tau_{xz} dz = -\bar{D} \frac{\partial}{\partial x} \nabla^2 w, \quad Q_y = \int_{-h/2}^{h/2} \tau_{yz} dz = -\bar{D} \frac{\partial}{\partial y} \nabla^2 w, \quad (8)$$

$$V_x = Q_x + \frac{\partial M_{xy}}{\partial y}, \quad V_y = Q_y + \frac{\partial M_{xy}}{\partial x}. \quad (9)$$

在上式中 $\bar{D} = \int_{-h/2}^{h/2} \frac{E(z)(z - z_0)^2}{1 - \nu^2} dz$ 为功能梯度板的等效弯曲刚度, w 为板的振型函数, $\overline{\rho h} = \int_{-h/2}^{h/2} \rho(z) dz$ 为板单位面积的密度, ω 为板的固有频率, M_x 和 M_y, M_{xy}, Q_x 和 Q_y, V_x 和 V_y 分别为板单位宽度上的弯矩、扭矩、横向剪力以及等效横向剪力.

1.3 将基本方程导入 Hamilton 体系

上小节中已经得到了功能梯度板自由振动的控制方程,本小节将从控制方程出发,将其导入 Hamilton 体系.

由式(6)的第 3 式和式(9)可得

$$\frac{\partial V_x}{\partial x} + \frac{\partial V_y}{\partial y} - 2 \frac{\partial M_{xy}}{\partial x \partial y} + \overline{\rho h \omega^2} w = 0. \quad (10)$$

令

$$\frac{\partial w}{\partial y} = \theta, \quad (11)$$

则式(7)的第 2 式可写为

$$\frac{\partial \theta}{\partial y} = -\nu \frac{\partial^2 w}{\partial x^2} - \frac{M_y}{\bar{D}}, \quad (12)$$

而式(7)的第 3 式可写为

$$M_{xy} = M_{yx} = -\bar{D}(1-\nu) \frac{\partial \theta}{\partial x}. \quad (13)$$

由式(7)的第 2、第 3 式和式(8)、式(9)的第 1 式、式(10),可得

$$\frac{\partial V_y}{\partial y} = \bar{D}(1-\nu^2) \frac{\partial^4 w}{\partial x^4} - \nu \frac{\partial^2 M_y}{\partial x^2} - \overline{\rho h \omega^2} w. \quad (14)$$

由式(6)的第 2 式、式(9)的第 2 式和式(13),可得

$$\frac{\partial M_y}{\partial y} = V_y + 2\bar{D}(1-\nu) \frac{\partial^2 \theta}{\partial x^2}. \quad (15)$$

再令 $T_y = -V_y$, 把式(11)、(14)和(15)写成如下的矩阵形式:

$$\frac{\partial \mathbf{Z}}{\partial y} = \mathbf{H}\mathbf{Z}, \quad (16)$$

其中

$$\mathbf{H} = \begin{bmatrix} \mathbf{F} & \mathbf{G} \\ \mathbf{Q} & -\mathbf{F}^T \end{bmatrix}, \quad \mathbf{Q} = \begin{bmatrix} \overline{\rho h \omega^2} - \bar{D}(1-\nu^2) \partial^4 / \partial x^4 & 0 \\ 0 & 2\bar{D}(1-\nu) \partial^2 / \partial x^2 \end{bmatrix},$$

$$\mathbf{F} = \begin{bmatrix} 0 & 1 \\ -\nu \partial^2 / \partial x^2 & 0 \end{bmatrix}, \quad \mathbf{G} = \begin{bmatrix} 0 & 0 \\ 0 & -1/\bar{D} \end{bmatrix}, \quad \mathbf{Z} = [w, \theta, T_y, M_y]^T$$

是功能梯度板自由振动的状态向量. \mathbf{H} 满足 $\mathbf{H}^T = \mathbf{J}\mathbf{H}\mathbf{J}$, 为 Hamilton 算子矩阵, 这里 $\mathbf{J} = \begin{bmatrix} \mathbf{0} & \mathbf{I}_2 \\ -\mathbf{I}_2 & \mathbf{0} \end{bmatrix}$ 是单位辛矩阵, \mathbf{I}_2 是二阶单位矩阵. 式(16)即为功能梯度板自由振动问题的 Hamilton 对偶方程.

2 基于 Hamilton 体系的功能梯度矩形板自由振动问题求解

2.1 对边简支功能梯度矩形板

经过以上推导,已经将功能梯度板自由振动问题导入到 Hamilton 体系当中.下面对式(16),即功能梯度板自由振动问题的 Hamilton 对偶方程进行求解.

基于辛几何中的分离变量法,令

$$\mathbf{Z} = \mathbf{X}(x)Y(y), \quad (17)$$

其中 $\mathbf{X}(x) = [w(x), \theta(x), T_y(x), M_y(x)]^T$ 是仅与 x 有关的向量, $Y(y)$ 是仅与 y 有关的函数.

将式(17)代入式(16)中得

$$\frac{dY(y)}{dy} = \mu Y(y), \quad (18)$$

相应的本征方程为

$$\mathbf{H}\mathbf{X}(x) = \mu\mathbf{X}(x), \quad (19)$$

其中 μ 为本征方程待求的本征值, $\mathbf{X}(x)$ 为 μ 对应的本征向量.

对于 $x = 0$ 和 $x = a$ 边简支的功能梯度矩形板, x 方向的边界条件为

$$w|_{x=0,a} = 0, M_x|_{x=0,a} = 0. \quad (20)$$

将式(20)代入式(19)便可求出其本征值与本征向量,其本征值为

$$\mu_{\pm m}^{(1)} = \pm \sqrt{\left(\frac{m\pi}{a}\right)^2 - R}, \mu_{\pm m}^{(2)} = \pm \sqrt{\left(\frac{m\pi}{a}\right)^2 + R}, \quad (21)$$

与本征值 $\mu_m^{(1)}$ 对应的本征向量为

$$\mathbf{X}_m^{(1)}(x) = \begin{bmatrix} \sin(\alpha_m x) \\ \mu_m^{(1)} \sin(\alpha_m x) \\ \bar{D}\mu_m^{(1)} [(\nu - 2)\alpha_m^2 + (\mu_m^{(1)})^2] \sin(\alpha_m x) \\ \bar{D}(\nu\alpha_m^2 - (\mu_m^{(1)})^2) \sin(\alpha_m x) \end{bmatrix}, \quad (22)$$

而与本征值 $\mu_m^{(2)}$ 对应的本征向量为

$$\mathbf{X}_m^{(2)}(x) = \begin{bmatrix} \sin(\alpha_m x) \\ \mu_m^{(2)} \sin(\alpha_m x) \\ \bar{D}\mu_m^{(2)} [(\nu - 2)\alpha_m^2 + (\mu_m^{(2)})^2] \sin(\alpha_m x) \\ \bar{D}[\nu\alpha_m^2 - (\mu_m^{(2)})^2] \sin(\alpha_m x) \end{bmatrix}, \quad (23)$$

其中 $R = \omega\sqrt{\rho h/\bar{D}}$, $\alpha_m = m\pi/a$, $m = 1, 2, 3, \dots$.

同理,将 $\mathbf{X}_m^{(1)}(x)$ 和 $\mathbf{X}_m^{(2)}(x)$ 中的 $\mu_m^{(1)}$ 和 $\mu_m^{(2)}$ 分别替换为 $\mu_{-m}^{(1)}$ 和 $\mu_{-m}^{(2)}$, 便可得到与本征值 $\mu_{-m}^{(1)}$ 和 $\mu_{-m}^{(2)}$ 分别对应的本征向量 $\mathbf{X}_{-m}^{(1)}(x)$ 和 $\mathbf{X}_{-m}^{(2)}(x)$.

由式(18)可得

$$\begin{cases} Y_m^{(1)} = C_m^{(1)} e^{\mu_m^{(1)}y}, Y_{-m}^{(1)} = C_{-m}^{(1)} e^{\mu_{-m}^{(1)}y}, \\ Y_m^{(2)} = C_m^{(2)} e^{\mu_m^{(2)}y}, Y_{-m}^{(2)} = C_{-m}^{(2)} e^{\mu_{-m}^{(2)}y}. \end{cases} \quad (24)$$

于是状态向量 \mathbf{Z} 可以展开成

$$\mathbf{Z} = \sum_{m=1,2,3,\dots}^{\infty} (C_m^{(1)} e^{\mu_m^{(1)}y} \mathbf{X}_m^{(1)} + C_{-m}^{(1)} e^{\mu_{-m}^{(1)}y} \mathbf{X}_{-m}^{(1)} + C_m^{(2)} e^{\mu_m^{(2)}y} \mathbf{X}_m^{(2)} + C_{-m}^{(2)} e^{\mu_{-m}^{(2)}y} \mathbf{X}_{-m}^{(2)}), \quad (25)$$

则状态向量中的振型函数 w 为

$$w = \sum_{m=1,2,3,\dots}^{\infty} (C_m^{(1)} e^{\mu_m^{(1)}y} + C_{-m}^{(1)} e^{\mu_{-m}^{(1)}y} + C_m^{(2)} e^{\mu_m^{(2)}y} + C_{-m}^{(2)} e^{\mu_{-m}^{(2)}y}) \sin(\alpha_m x), \quad (26)$$

其中 $C_m^{(1)}$, $C_{-m}^{(1)}$, $C_m^{(2)}$, $C_{-m}^{(2)}$ 为待求系数.通过引入板在 y 方向的边界条件,便可得到板的频率方程,从而得到相应的解析解.

2.2 非 Lévy 型功能梯度矩形板

本小节聚焦典型的非 Lévy 型功能梯度矩形板,所考虑的四边固支板自由振动问题的辛叠加方法如图 3 所示,其中坐标系的原点 O 位于板的左上角,板的长度为 a 、宽度为 b .这里 S 表示简支、C 表示固支,并从 $x = 0$ 边开始以逆时针方向通过字母对板命名.CCCC 板问题被拆分成子问题 1 和子问题 2,利用辛方法分别对子问题 1 和 2 进行求解,而后叠加求出原问题的解.

子问题 1 和 2 均为 SSSS 型边界,而原问题的边界条件为在四条边上分别满足位移、转角为零,即

$$\begin{cases} w|_{x=0,a} = w|_{y=0,b} = 0, \\ \theta|_{x=0,a} = \theta|_{y=0,b} = 0. \end{cases} \quad (27)$$

而两个子问题原本满足

$$w|_{x=0,a} = w|_{y=0,b} = 0. \tag{28}$$

为了使子问题叠加后与原问题等价,需要对子问题 1 的 $y = 0$ 和 $y = b$ 边分别施加 $\sum_{m=1,2,3,\dots}^{\infty} E_m \sin(\alpha_m x)$ 和 $\sum_{m=1,2,3,\dots}^{\infty} F_m \sin(\alpha_m x)$ 表示的弯矩作用,对子问题 2 的 $x = 0$ 和 $x = a$ 边分别施加 $\sum_{n=1,2,3,\dots}^{\infty} G_n \sin(\beta_n y)$ 和 $\sum_{n=1,2,3,\dots}^{\infty} H_n \sin(\beta_n y)$ 表示的弯矩作用, E_m, F_m, G_n, H_n 为待求系数, $\alpha_m = m\pi/a, \beta_n = n\pi/b$, 其中 $m = 1, 2, 3, \dots, n = 1, 2, 3, \dots$.

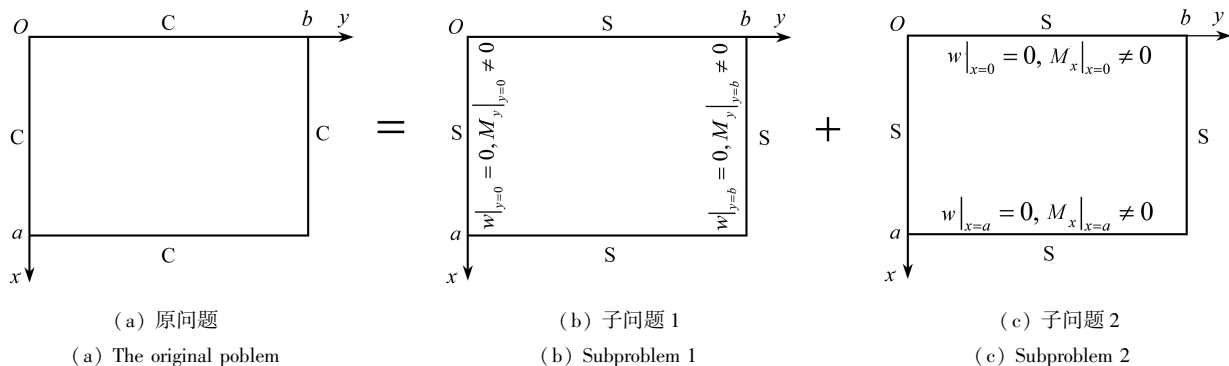


图 3 CCCC 板辛叠加示意图

Fig. 3 Schematic diagram of symplectic superposition for a CCCC plate

对于子问题 1 而言,当在 $y = 0$ 和 $y = b$ 边上强加弯矩时,对应的边界条件如下:

$$\begin{cases} w|_{y=0} = 0, M_y|_{y=0} = \sum_{m=1,2,3,\dots}^{\infty} E_m \sin(\alpha_m x), \\ w|_{y=b} = 0, M_y|_{y=b} = \sum_{m=1,2,3,\dots}^{\infty} F_m \sin(\alpha_m x). \end{cases} \tag{29}$$

将式(29)代入式(25)即可求得由未知系数 E_m 和 F_m 表达的子问题 1 的无量纲解:

$$\begin{aligned} \frac{w_1(\bar{x}, \bar{y})}{a} = & \sum_{m=1,2,3,\dots}^{\infty} \frac{\sin(m\pi\bar{x})}{2\bar{\omega}} \{ [\cosh(\phi\zeta_m\bar{y}) - \cosh(\phi\eta_m\bar{y}) - \\ & \coth(\phi\zeta_m) \sinh(\phi\zeta_m\bar{y}) + \coth(\phi\eta_m) \sinh(\phi\eta_m\bar{y})] \bar{E}_m + \\ & [\cosh(\phi\zeta_m) \sinh(\phi\zeta_m\bar{y}) - \operatorname{csch}(\phi\eta_m) \sinh(\phi\eta_m\bar{y})] \bar{F}_m \}, \end{aligned} \tag{30}$$

其中

$$\begin{aligned} \bar{x} = x/a, \bar{y} = y/b, \phi = b/a, \bar{E}_m = bE_m/\bar{D}, \bar{F}_m = bF_m/\bar{D}, \\ \bar{\omega} = \omega a^2 \sqrt{\rho h/\bar{D}}, \zeta_m = \sqrt{m^2 \pi^2 - \bar{\omega}}, \eta_m = \sqrt{m^2 \pi^2 + \bar{\omega}}. \end{aligned}$$

对于子问题 2 而言,利用类似于子问题 1 的求解方法便可得到由未知系数 G_n 和 H_n 表达的无量纲解:

$$\begin{aligned} \frac{w_2(\bar{x}, \bar{y})}{b} = & \sum_{n=1,2,3,\dots}^{\infty} \frac{1}{2\hat{\omega}} \sin(n\pi\bar{y}) \{ [\cosh(\bar{\phi}\xi_n\bar{x}) - \\ & \cosh(\bar{\phi}\eta_n\bar{x}) - \coth(\bar{\phi}\xi_n) \sinh(\bar{\phi}\xi_n\bar{x}) + \coth(\bar{\phi}\eta_n) \sinh(\bar{\phi}\eta_n\bar{x})] \bar{G}_n + \\ & [\operatorname{csch}(\bar{\phi}\xi_n) \sinh(\bar{\phi}\xi_n\bar{x}) - \operatorname{csch}(\bar{\phi}\eta_n) \sinh(\bar{\phi}\eta_n\bar{x})] \bar{H}_n \}, \end{aligned} \tag{31}$$

其中

$$\begin{aligned} \bar{x} = x/a, \bar{y} = y/b, \bar{\phi} = a/b, \bar{G}_n = bG_n/\bar{D}, \bar{H}_n = bH_n/\bar{D}, \\ \hat{\omega} = \omega b^2 \sqrt{\rho h/\bar{D}}, \xi_n = \sqrt{n^2 \pi^2 - \hat{\omega}}, \eta_n = \sqrt{n^2 \pi^2 + \hat{\omega}}. \end{aligned}$$

在得到子问题 1 和子问题 2 的解答后,便可将两个子问题进行叠加,叠加后需分别满足各个边转角为零的条件,即

$$\begin{cases} \sum_{i=1}^2 \frac{\partial w_i}{\partial x} \Big|_{x=0,a} = 0, \\ \sum_{i=1}^2 \frac{\partial w_i}{\partial y} \Big|_{y=0,b} = 0. \end{cases} \quad (32)$$

将式(30)、(31)代入式(32),并将相应函数展开为对应的正弦级数,利用正交性便可形成包含 E_m, H_m, G_n 和 H_n 的方程组,其中 $m = 1, 2, 3, \dots, n = 1, 2, 3, \dots$. CCCC 功能梯度矩形板四条边的弯矩不能全为零,即 E_m, F_m, G_n 和 H_n 存在非零解,这就要求所得方程组的系数矩阵行列式为零.由此,便给出了求解固有频率的方程,将得到的固有频率解代回上述方程组,得到 E_m, F_m, G_n 和 H_n 的非零解,进一步代入式(30)和(31),叠加即可得到问题的振型解.需要注意,在实际计算中需取无穷联立方程的有限项进行求解,为方便起见,本文对于四组未知数取相同的项数 N .

对于 CCCC 板问题和 CCSS 板问题,只需在 CCCC 问题基础上减少相应的约束即可:去掉子问题 1 中 $y = b$ 边上强加的弯矩,不再限制 $y = b$ 边上的转角为零,同时去掉相关方程和含 F_m 的项,即可获得 CCCC 板问题的解.进一步去掉子问题 2 中 $x = a$ 边上强加的弯矩,不再限制 $x = a$ 边上的转角为零,同时去掉相关方程和含 H_n 的项,即可获得 CCSS 板问题的解.

3 数值算例与讨论

由上文可知,通过辛叠加方法求解 CCCC、CCCS、CCSS 等功能梯度矩形板的固有频率时得到的方程具有无穷项,而在实际计算中,只需根据精度要求取有限项计算,因此首先需要进行收敛性分析.本文在 $k = 20$ 的情况下分别研究了 $b/a = 1$ 和 $b/a = 2$ 时功能梯度矩形板解的收敛性,其中陶瓷材料采用 Al_2O_3 ,其弹性模量为 380 GPa,密度为 3 800 kg/m^3 ,Poisson 比 $\nu = 0.3$;金属材料采用 Al,其弹性模量为 70 GPa,密度为 2 707 kg/m^3 ,Poisson 比 $\nu = 0.3$; $D_c = E_c h^3 / (12(1 - \nu^2))$ 为板全为陶瓷材料时的抗弯刚度.表 1 给出了 CCCC 功能梯度矩形板的前十阶无量纲固有频率参数 $\omega a^2 \sqrt{\rho_c h / D_c}$ 的收敛性分析.可以看出,辛叠加方法具有较快的收敛性,当 N 取 20 时,结果已经收敛到了 5 位有效数字(表中加粗数据).后续计算中将 N 取 30 以确保所有结果收敛到 5 位有效数字.

表 1 CCCC 功能梯度矩形板的前十阶无量纲固有频率参数 $\omega a^2 \sqrt{\rho_c h / D_c}$ 的收敛性研究

Table1 Convergence study of the first ten non-dimensional natural frequency parameters

$\omega a^2 \sqrt{\rho_c h / D_c}$ of CCCC functionally graded rectangular plates

b/a	N	mode									
		1st	2nd	3rd	4th	5th	6th	7th	8th	9th	10th
1	5	21.724	44.299	44.299	65.274	79.437	79.786	99.522	99.522	127.00	127.00
	10	21.725	44.309	44.309	65.331	79.437	79.813	99.610	99.610	127.09	127.09
	20	21.725	44.309	44.309	65.332	79.437	79.814	99.613	99.613	127.09	127.09
	30	21.725	44.309	44.309	65.332	79.437	79.814	99.613	99.613	127.09	127.09
	40	21.725	44.309	44.309	65.332	79.437	79.814	99.613	99.613	127.09	127.09
	50	21.725	44.309	44.309	65.332	79.437	79.814	99.613	99.613	127.09	127.09
2	5	14.837	19.197	27.008	38.073	38.622	42.865	50.208	52.530	60.423	74.227
	10	14.838	19.214	27.027	38.232	38.627	42.909	50.268	52.671	60.843	70.241
	20	14.838	19.214	27.028	38.234	38.628	42.910	50.273	52.676	60.850	70.247
	30	14.838	19.214	27.028	38.234	38.628	42.910	50.273	52.676	60.850	70.247
	40	14.838	19.214	27.028	38.234	38.628	42.910	50.273	52.676	60.850	70.247
	50	14.838	19.214	27.028	38.234	38.628	42.910	50.273	52.676	60.850	70.247

表 2—表 4 分别计算了不同体积分数指数和长宽比下 CCCC、CCCS 和 CCSS 板的无量纲固有频率参数.由于没有可供对比的解析解,将所得解析解与文献中的部分数值解以及精细有限元分析结果进行对比,其中

有限元结果由 ABAQUS 软件计算得到,其模型的设置如下:采用 S4R 单元,网格尺寸为 $a/200$ 。通过对比算例可见,本文的计算结果与其他方法所得结果几乎一致,从而证明了本文方法的正确性。图 4—图 6 给出了 $k = 20$ 时,3 种边界下功能梯度方板的前十阶振型,本文结果与精细有限元分析结果完全一致,进一步说明了本文求解的精确性。

表 2 CCCC 功能梯度矩形板的前十阶无量纲固有频率参数 $\omega a^2 \sqrt{\rho_c h/D_c}$

Table 2 The first ten non-dimensional natural frequency parameters

$\omega a^2 \sqrt{\rho_c h/D_c}$ of CCCC functionally graded rectangular plates

b/a	k	method	mode									
			1st	2nd	3rd	4th	5th	6th	7th	8th	9th	10th
1	0	present	35.985	73.394	73.394	108.22	131.58	132.20	165.00	165.00	210.52	210.52
		FEM	35.987	73.405	73.405	108.23	131.63	132.25	165.04	165.04	210.64	210.64
		ref. [24]	35.983	73.384	73.384	108.19	131.57					
	0.2	present	33.394	68.108	68.108	100.42	122.10	122.68	153.12	153.12	195.36	195.36
		FEM	33.402	68.128	68.128	100.45	122.16	122.74	153.18	153.18	195.50	195.50
	0.5	present	30.470	62.146	62.146	91.632	111.42	111.94	139.71	139.71	178.26	178.26
		FEM	30.475	62.160	62.160	91.650	111.46	111.99	139.76	139.76	178.37	178.37
		ref. [24]	30.468	62.137	62.137	91.611	111.41					
	1	present	27.457	55.999	55.999	82.569	100.40	100.87	125.89	125.89	160.63	160.63
		FEM	27.459	56.008	56.008	82.581	100.43	100.91	125.93	125.93	160.72	160.72
		ref. [24]	27.454	55.991	55.991	82.548	100.38					
	2	present	24.963	50.913	50.913	75.070	91.277	91.710	114.46	114.46	146.04	146.04
		FEM	24.964	50.921	50.921	75.080	91.308	91.741	114.49	114.49	146.12	146.12
		ref. [24]	24.961	50.904	50.904	75.048	91.262					
	5	present	23.669	48.273	48.273	71.178	86.545	86.955	108.53	108.53	138.47	138.47
		FEM	23.670	48.280	48.280	71.186	86.573	86.984	108.55	108.55	138.55	138.55
	10	present	22.920	46.746	46.746	68.926	83.807	84.205	105.09	105.09	134.09	134.09
		FEM	22.921	46.752	46.752	68.933	83.833	84.231	105.12	105.12	134.16	134.16
20	present	21.725	44.309	44.309	65.332	79.437	79.814	99.613	99.613	127.09	127.09	
	FEM	21.725	44.313	44.313	65.336	79.458	79.835	99.631	99.631	127.16	127.16	
2	0	present	24.578	31.826	44.770	63.331	63.983	71.076	83.273	87.253	100.79	116.36
		FEM	24.579	31.827	44.773	63.338	63.996	71.088	83.284	87.269	100.80	116.39
	0.2	present	22.808	29.534	41.546	58.770	58.770	65.958	77.276	80.969	93.533	107.98
		FEM	22.814	29.541	41.555	58.785	59.395	65.977	77.296	80.995	93.557	108.02
	0.5	present	20.811	26.949	37.909	53.625	54.178	60.184	70.511	73.881	85.345	98.525
		FEM	20.816	26.953	37.914	53.635	54.192	60.197	70.525	73.899	85.361	98.558
	1	present	18.753	24.283	34.159	48.321	48.819	54.231	63.537	66.573	76.904	88.780
		FEM	18.754	24.285	34.162	48.327	48.829	54.240	63.546	66.586	76.914	88.805
	2	present	17.050	22.078	31.057	43.932	44.385	49.305	57.766	60.527	69.919	80.717
		FEM	17.051	22.079	31.059	43.937	44.394	49.313	57.774	60.538	69.928	80.739
	5	present	16.166	20.933	29.446	41.655	42.084	46.749	54.771	57.389	66.294	76.532
		FEM	16.167	20.934	29.448	41.659	42.091	46.756	54.778	57.399	66.302	76.552
	10	present	15.654	20.271	28.515	40.337	40.752	45.270	53.038	55.573	64.197	74.111
		FEM	15.656	20.272	28.516	40.341	40.759	45.276	53.044	55.582	64.203	74.129
	20	present	14.838	19.214	27.028	38.234	38.628	42.910	50.273	52.676	60.850	70.247
		FEM	14.839	19.214	27.029	38.236	38.633	42.914	50.276	52.682	60.853	70.261

图 7 给出了 3 种边界下、不同长宽比的功能梯度矩形板的基频参数随着体积分数 k 的变化。可以看出,

随着 k 的增加所有边界下板的基频参数均降低,这是由于 k 的增加使板的抗弯刚度和密度减小,但刚度变化对基频的影响要强于密度变化对基频的影响.此外发现, $b/a = 2$ 时 CCCC 板与 CCCS 板的基频相差很小,这是由于 CCCS 板简支端的边长为 a , 当固支端替换为简支端对基频影响较小.

上述结果不仅可作为其他数值方法对比的基准,还有望为实际工程中功能梯度板的初步设计提供参考.

表 3 CCCS 功能梯度矩形板的前十阶无量纲固有频率参数 $\omega a^2 \sqrt{\rho_c h/D_c}$

Table 3 The first ten non-dimensional natural frequency parameters

$\omega a^2 \sqrt{\rho_c h/D_c}$ of CCCS functionally graded rectangular plates

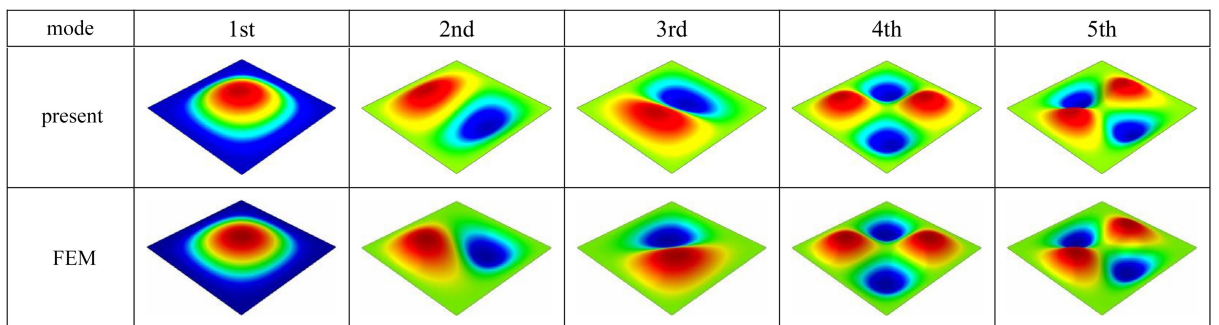
b/a	k	method	mode									
			1st	2nd	3rd	4th	5th	6th	7th	8th	9th	10th
1	0	present	31.826	63.331	71.076	100.79	116.36	130.35	151.89	159.48	189.77	209.32
		FEM	31.827	63.338	71.088	100.80	116.39	130.40	151.92	159.52	189.86	209.37
	0.2	present	29.534	58.770	65.958	93.533	107.98	120.96	140.95	147.99	176.10	194.25
		FEM	29.541	58.785	65.977	93.557	108.02	121.02	141.00	148.05	176.21	194.32
	0.5	present	26.949	53.625	60.184	85.346	98.525	110.37	128.62	135.04	160.69	177.24
		FEM	26.953	53.635	60.197	85.361	98.558	110.42	128.65	135.08	160.78	177.30
	1	present	24.283	48.321	54.231	76.904	88.780	99.458	115.89	121.68	144.79	159.71
		FEM	24.285	48.327	54.240	76.914	88.805	99.493	115.92	121.71	144.87	159.75
	2	present	22.078	43.932	49.306	69.919	80.717	90.424	105.37	110.63	131.64	145.21
		FEM	22.079	43.937	49.313	69.928	80.739	90.456	105.39	110.66	131.71	145.24
5	present	20.933	41.655	46.749	66.294	76.532	85.736	99.905	104.89	124.82	137.68	
	FEM	20.934	41.659	46.756	66.302	76.552	85.765	99.924	104.92	124.88	137.71	
10	present	20.271	40.337	45.270	64.197	74.111	83.024	96.744	101.57	120.87	133.32	
	FEM	20.272	40.341	45.276	64.203	74.129	83.050	96.762	101.60	120.93	133.35	
20	present	19.214	38.234	42.910	60.850	70.247	78.695	91.700	96.278	114.57	126.37	
	FEM	19.214	38.236	42.914	60.853	70.261	78.716	91.712	96.296	114.62	126.39	
2	0	present	24.143	30.249	41.751	58.852	63.741	70.141	81.291	81.367	97.545	109.11
		FEM	24.145	30.251	41.753	58.858	63.754	70.153	81.302	81.380	97.557	109.14
	0.2	present	22.404	28.071	38.744	54.614	59.151	65.090	75.437	75.507	90.521	101.25
		FEM	22.411	28.077	38.752	54.627	59.171	65.109	75.457	75.530	90.544	101.29
	0.5	present	20.443	25.613	35.352	49.833	53.973	59.392	68.833	68.897	82.596	92.390
		FEM	20.448	25.618	35.357	49.841	53.987	59.406	68.847	68.913	82.611	92.419
	1	present	18.421	23.080	31.856	44.904	48.634	53.518	62.025	62.083	74.427	83.252
		FEM	18.422	23.081	31.858	44.909	48.644	53.527	62.034	62.093	74.436	83.273
	2	present	16.748	20.984	28.962	40.826	44.217	48.657	56.392	56.444	75.691	75.691
		FEM	16.749	20.985	28.964	40.830	44.226	48.665	56.399	56.453	75.675	75.709
5	present	15.879	19.896	27.461	38.709	41.925	46.134	53.468	53.518	64.159	71.766	
	FEM	15.881	19.897	27.462	38.713	41.932	46.141	53.474	53.526	64.166	71.783	
10	present	15.377	19.266	26.592	37.485	40.598	44.675	51.777	51.825	62.129	69.496	
	FEM	15.379	19.267	26.593	37.487	40.605	44.681	51.782	51.832	62.135	69.511	
20	present	14.575	18.262	25.206	35.530	38.482	42.345	49.077	49.123	58.890	65.873	
	FEM	14.576	18.262	25.206	35.531	38.487	42.349	49.080	49.127	58.893	65.884	

表 4 CCSS 功能梯度矩形板的前十阶无量纲固有频率参数 $\omega a^2 \sqrt{\rho_c h/D_c}$

Table 4 The first ten non-dimensional natural frequency parameters

$\omega a^2 \sqrt{\rho_c h/D_c}$ of CCSS functionally graded rectangular plates

b/a	k	method	mode									
			1st	2nd	3rd	4th	5th	6th	7th	8th	9th	10th
1	0	present	27.054	60.538	60.786	92.836	114.56	114.70	145.78	146.08	188.46	188.55
		FEM	27.055	60.546	60.793	92.846	114.59	114.74	145.81	146.11	188.56	188.65
	0.2	present	25.106	56.179	56.409	86.150	106.31	106.44	135.28	135.56	174.89	174.97
		FEM	25.112	56.193	56.423	86.171	106.35	106.49	135.33	135.61	175.00	175.09
	0.5	present	22.908	51.261	51.471	78.609	97.000	97.125	123.44	123.69	159.58	159.66
		FEM	22.912	51.270	51.480	78.622	97.034	97.159	123.47	123.73	159.67	159.75
	1	present	20.642	46.191	46.380	70.834	87.406	87.519	111.23	111.46	143.79	143.86
		FEM	20.643	46.197	46.385	70.842	87.432	87.544	111.25	111.48	143.87	143.94
	2	present	18.767	41.995	42.167	64.400	79.468	79.570	101.13	101.34	130.73	130.80
		FEM	18.768	42.000	42.172	64.407	79.490	79.592	101.15	101.36	130.80	130.87
5	present	17.794	39.818	39.981	61.061	75.347	75.444	95.885	96.082	124.02	124.02	
	FEM	17.795	39.822	39.985	61.067	75.368	75.465	95.904	96.101	123.96	124.02	
10	present	17.231	38.558	38.716	59.130	72.964	73.058	92.851	93.042	120.04	120.09	
	FEM	17.232	38.562	38.720	59.134	72.982	73.076	92.868	93.059	120.09	120.15	
20	present	16.333	36.548	36.698	56.047	69.159	69.249	88.010	88.191	113.78	113.83	
	FEM	16.333	36.550	36.700	56.049	69.174	69.263	88.022	88.203	113.83	113.88	
2	0	present	17.769	25.198	37.973	52.342	55.988	59.586	71.882	79.117	89.337	106.65
		FEM	17.770	25.199	37.975	52.350	55.994	59.593	71.889	79.130	89.347	106.68
	0.2	present	16.489	23.383	35.239	48.573	51.956	55.295	66.705	73.419	82.904	98.968
		FEM	16.495	23.389	35.246	48.587	51.969	55.309	66.721	73.441	82.923	99.012
	0.5	present	15.046	21.336	32.154	44.321	47.408	50.454	60.866	66.992	75.646	90.304
		FEM	15.050	21.340	32.159	44.331	47.416	50.464	60.876	67.008	75.658	90.338
	1	present	13.558	19.226	28.973	39.937	42.719	45.464	54.846	60.366	68.164	81.372
		FEM	13.559	19.227	28.975	39.943	42.724	45.470	54.852	60.376	68.172	81.399
	2	present	12.326	17.480	26.342	36.310	38.839	41.334	49.864	54.883	61.973	73.981
		FEM	12.327	17.481	26.344	36.315	38.843	41.339	49.869	54.892	61.979	74.005
5	present	11.687	16.574	24.976	34.427	36.825	39.191	47.279	52.038	58.760	70.146	
	FEM	11.688	16.574	24.978	34.432	36.829	39.196	47.283	52.046	58.765	70.167	
10	present	11.318	16.049	24.186	33.338	35.660	37.952	45.783	50.391	56.901	67.927	
	FEM	11.319	16.050	24.187	33.342	35.663	37.955	45.787	50.399	56.905	67.947	
20	present	10.727	15.212	22.925	31.600	33.801	35.973	43.396	47.764	53.934	64.385	
	FEM	10.729	15.213	22.925	31.603	33.802	35.975	43.398	47.769	53.936	64.401	



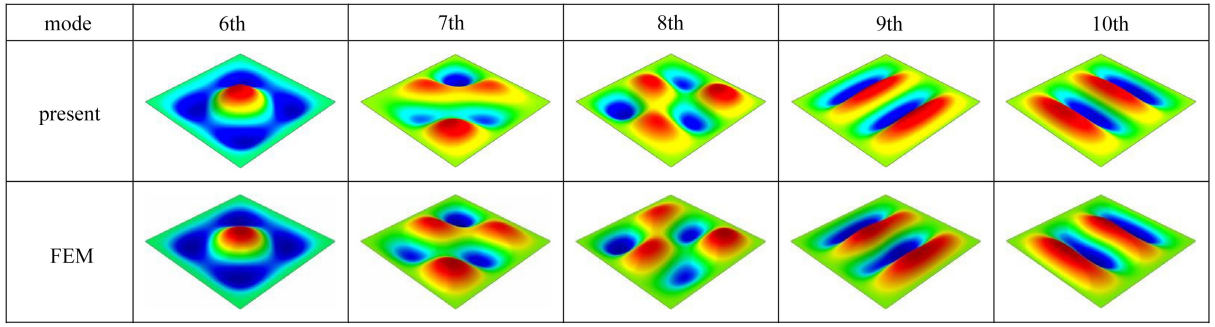


图4 CCCC功能梯度方板的前十阶振型

Fig. 4 The first ten mode shapes of a CCCC functionally graded square plate

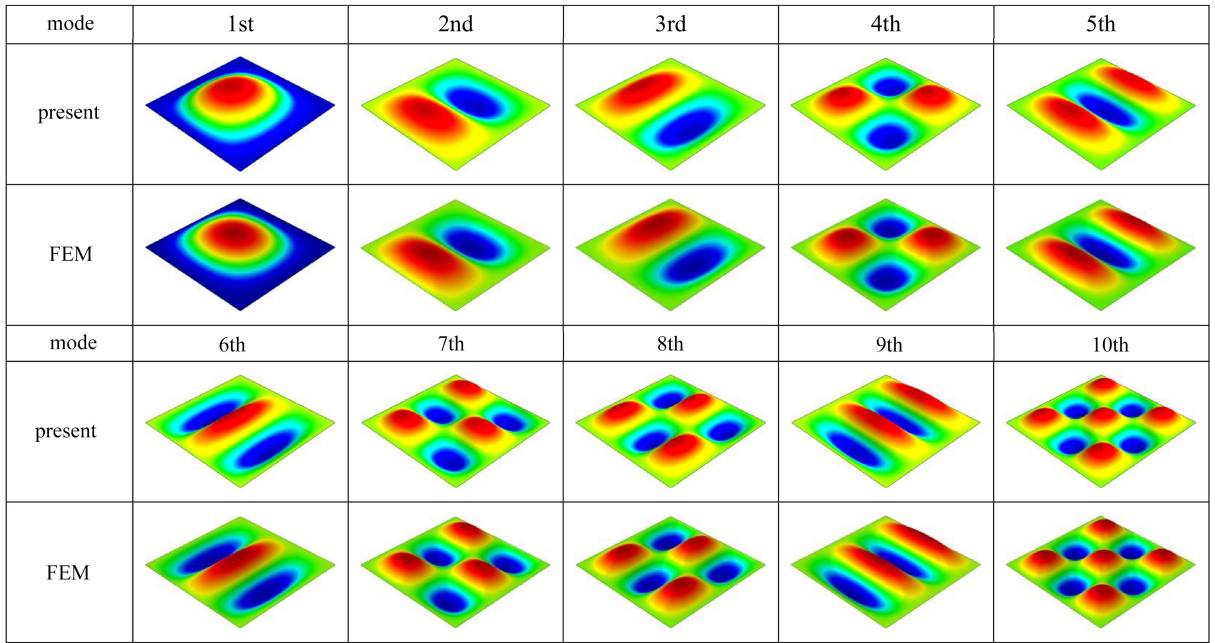
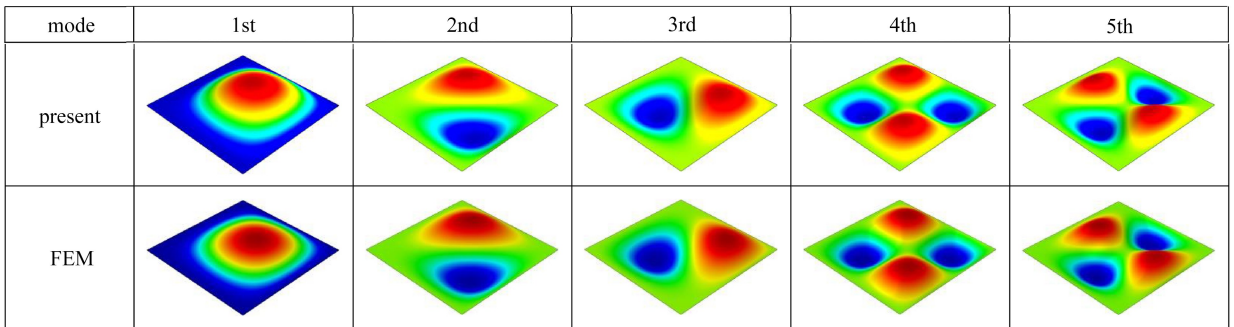


图5 CCCS功能梯度方板的前十阶振型

Fig. 5 The first ten mode shapes of a CCCS functionally graded square plate



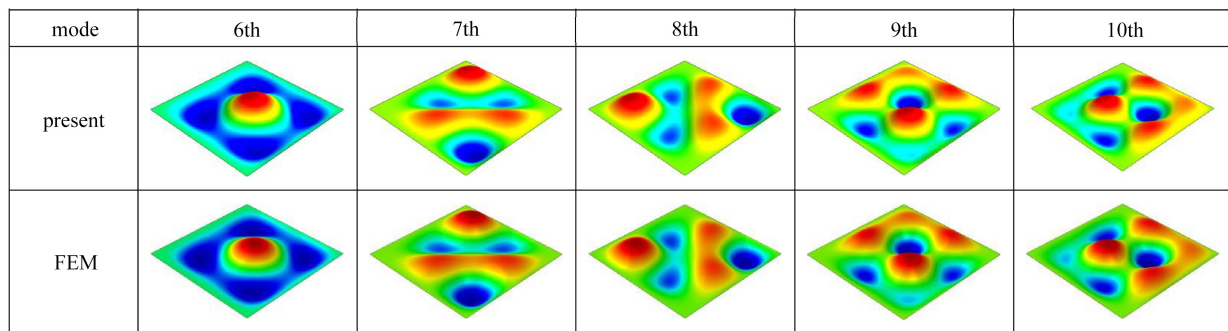


图 6 CCSS 功能梯度方板的前十阶振型

Fig. 6 The first ten mode shapes of a CCSS functionally graded square plate

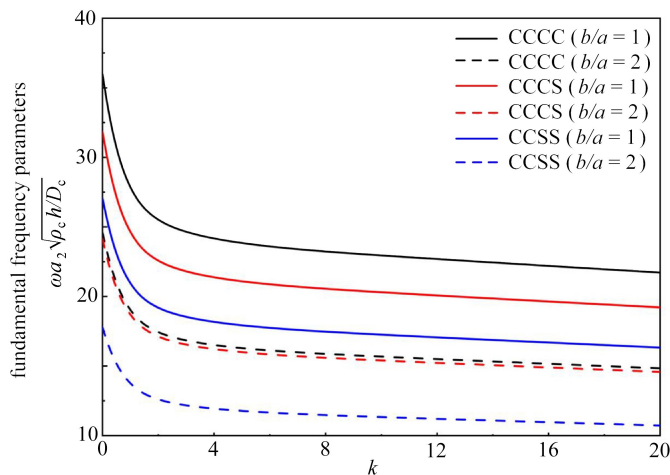


图 7 不同边界和长宽比下功能梯度矩形板的基频参数随体积分数指数 k 变化

Fig. 7 Fundamental frequency parameters vs. volume fraction index k of functionally graded rectangular plates with different boundaries and aspect ratios

4 结 论

本文在 Hamilton 体系下解析求解了非 Lévy 型功能梯度矩形板的自由振动问题,基于经典薄板理论,利用物理中性面的概念建立了功能梯度板自由振动问题的 Hamilton 对偶方程,实现了由传统的欧式空间向辛空间的转换,进一步利用在传统求解体系下难以使用的分离变量、辛本征展开等数学手段进行求解.对于含非 Lévy 型边界的功能梯度矩形板自由振动问题,以四边固支板为例,采用以 Hamilton 体系为基础的辛叠加方法,将原问题拆分为两个易于求解的子问题.首先求解子问题,而后通过将子问题的解进行叠加得到原问题的解,并通过退化四边固支板的方程得到了其他简固支组合非 Lévy 型边界下功能梯度矩形板自由振动问题的解析解.在数值算例中,通过与文献和精细有限元数值结果进行对比,验证了本文方法的收敛性和正确性,同时还利用所得解析解研究了边界条件、材料分布和长宽比的影响.辛叠加方法求解过程中不需要假定试函数,兼备了辛方法理性和叠加法的规律性,可为复杂约束下板壳力学问题的求解提供一种新思路.

参考文献 (References):

[1] KOIZUMI M. The concept of FGM[J]. *Ceramic Transactions*, 1993, **34**: 3-10.
 [2] THAI H T, KIM S E. A review of theories for the modeling and analysis of functionally graded plates and shells [J]. *Composite Structures*, 2015, **128**: 70-86.
 [3] PINGULKAR P, SURESHA B. Free vibration analysis of laminated composite plates using finite element method[J]. *Polymers and Polymer Composites*, 2016, **24**(7): 529-538.

- [4] VINYAS M. A higher-order free vibration analysis of carbon nanotube-reinforced magneto-electro-elastic plates using finite element methods[J]. *Composites (Part B): Engineering*, 2019, **158**: 286-301.
- [5] CHEN M F, JIN G Y, YE T G, et al. An isogeometric finite element method for the in-plane vibration analysis of orthotropic quadrilateral plates with general boundary restraints[J]. *International Journal of Mechanical Sciences*, 2017, **133**: 846-862.
- [6] 李情, 陈莘莘. 基于重构边界光滑离散剪切间隙法的复合材料层合板自由振动分析[J]. *应用数学和力学*, 2022, **43**(10): 1123-1132. (LI Qing, CHEN Shenshen. Free vibration analysis of laminated composite plates based on the reconstructed edge-based smoothing DSG method[J]. *Applied Mathematics and Mechanics*, 2022, **43**(10): 1123-1132. (in Chinese))
- [7] BESKOS D E. Boundary element methods in dynamic analysis[J]. *Applied Mechanics Reviews*, 1987, **40**(1): 1-23.
- [8] NAJARZADEH L, MOVAHEDIAN B, AZHARI M. Free vibration and buckling analysis of thin plates subjected to high gradients stresses using the combination of finite strip and boundary element methods[J]. *Thin-Walled Structures*, 2018, **123**: 36-47.
- [9] CHEN J T, CHEN I L, CHEN K H, et al. A meshless method for free vibration analysis of circular and rectangular clamped plates using radial basis function[J]. *Engineering Analysis With Boundary Elements*, 2004, **28**(5): 535-545.
- [10] WANG J F, YANG J P, LAI S K, et al. Stochastic meshless method for nonlinear vibration analysis of composite plate reinforced with carbon fibers[J]. *Aerospace Science and Technology*, 2020, **105**: 105919.
- [11] YOUNG D. Vibration of rectangular plates by the Ritz method[J]. *Journal of Applied Mechanics; Transactions of the ASME*, 1950, **17**(4): 448-453.
- [12] LEISSA A W. The free vibration of rectangular plates[J]. *Journal of Sound and Vibration*, 1973, **31**(3): 257-293.
- [13] QIN B, ZHONG R, WU Q Y, et al. A unified formulation for free vibration of laminated plate through Jacobi-Ritz method[J]. *Thin-Walled Structures*, 2019, **144**: 106354.
- [14] 鲍四元, 邓子辰. 薄板弯曲自由振动问题的高精度近似解析解及改进研究[J]. *应用数学和力学*, 2016, **37**(11): 1169-1180. (BAO Siyuan, DENG Zichen. High-precision approximate analytical solutions for free bending vibrations of thin plates and an improvement [J]. *Applied Mathematics and Mechanics*, 2016, **37**(11): 1169-1180. (in Chinese))
- [15] 王永福, 漆文凯, 沈承, 等. 弹性约束边界条件下矩形蜂窝夹芯板的自由振动分析[J]. *应用数学和力学*, 2019, **40**(6): 583-594. (WANG Yongfu, QI Wenkai, SHEN Cheng, et al. Free vibration analysis of rectangular honeycomb-cored plates under elastically constrained boundary conditions [J]. *Applied Mathematics and Mechanics*, 2019, **40**(6): 583-594. (in Chinese))
- [16] WANG X, BERT C W. A new approach in applying differential quadrature to static and free vibrational analyses of beams and plates[J]. *Journal of Sound and Vibration*, 1993, **162**(3): 566-572.
- [17] TORNABENE F, LIVERANI A, CALIGIANA G. FGM and laminated doubly curved shells and panels of revolution with a free-form meridian: a 2-D GDQ solution for free vibrations[J]. *International Journal of Mechanical Sciences*, 2011, **53**(6): 446-470.
- [18] WANG Y, FENG C, YANG J, et al. Nonlinear vibration of FG-GPLRC dielectric plate with active tuning using differential quadrature method[J]. *Computer Methods in Applied Mechanics and Engineering*, 2021, **379**: 113761.
- [19] ZHANG C Y, JIN G Y, YE T G, et al. Harmonic response analysis of coupled plate structures using the dynamic stiffness method[J]. *Thin-Walled Structures*, 2018, **127**: 402-415.
- [20] AKSU G, ALI R. Free vibration analysis of stiffened plates using finite-difference method[J]. *Journal of Sound and Vibration*, 1976, **48**(1): 15-25.
- [21] QU W, HE H. A GFDM with supplementary nodes for thin elastic plate bending analysis under dynamic loading[J]. *Applied Mathematics Letters*, 2022, **124**: 107664.

- [22] HIEN T D, NOH H C. Stochastic isogeometric analysis of free vibration of functionally graded plates considering material randomness[J]. *Computer Methods in Applied Mechanics and Engineering*, 2017, **318**: 845-863.
- [23] KUMAR S, RANJAN V, JANA P. Free vibration analysis of thin functionally graded rectangular plates using the dynamic stiffness method[J]. *Composite Structures*, 2018, **197**: 39-53.
- [24] YIN S H, HALE J S, YU T T, et al. Isogeometric locking-free plate element: a simple first order shear deformation theory for functionally graded plates[J]. *Composite Structures*, 2014, **118**: 121-138.
- [25] THANG P T, LEE J. Free vibration characteristics of sigmoid-functionally graded plates reinforced by longitudinal and transversal stiffeners[J]. *Ocean Engineering*, 2018, **148**: 53-61.
- [26] JHA D K, KANT T, SINGH R K. Free vibration response of functionally graded thick plates with shear and normal deformations effects[J]. *Composite Structures*, 2013, **96**: 799-823.
- [27] KIM J, ZUR K K, REDDY J N. Bending, free vibration, and buckling of modified couples stress-based functionally graded porous micro-plates[J]. *Composite Structures*, 2019, **209**: 879-888.
- [28] 高祥雨, 王壮壮, 马连生. 功能梯度板弯曲和自由振动分析的简单精化板理论[J]. 固体力学学报, 2023, **44**(1): 96-108. (GAO Xiangyu, WANG Zhuangzhuang, MA Liansheng. A simple refined plate theory for bending and free vibration analysis of functionally graded plate[J]. *Chinese Journal of Solid Mechanics*, 2023, **44**(1): 96-108. (in Chinese))
- [29] BAFERANI A H, SAIDI A R, JOMEHZADEH E. An exact solution for free vibration of thin functionally graded rectangular plates[J]. *Proceedings of the Institution of Mechanical Engineers (Part C): Journal of Mechanical Engineering Science*, 2011, **225**(3): 526-536.
- [30] FARANGI M A A, SAIDI A R. Lévy type solution for free vibration analysis of functionally graded rectangular plates with piezoelectric layers[J]. *Smart Materials and Structures*, 2012, **21**(9): 094017.
- [31] DEMIRHAN P A, TASKIN V. Bending and free vibration analysis of Levy-type porous functionally graded plate using state space approach[J]. *Composites (Part B): Engineering*, 2019, **160**: 661-676.
- [32] HU Z, YANG Y, ZHOU C, et al. On the symplectic superposition method for new analytic free vibration solutions of side-cracked rectangular thin plates[J]. *Journal of Sound and Vibration*, 2020, **489**: 115695.
- [33] HU Z, ZHOU C, NI Z, et al. New symplectic analytic solutions for buckling of CNT reinforced composite rectangular plates[J]. *Composite Structures*, 2023, **303**: 116361.
- [34] XU D, XIONG S, MENG F, et al. An analytic model of transient heat conduction for bi-layered flexible electronic heaters by symplectic superposition[J]. *Micromachines*, 2022, **13**(10): 1627.
- [35] YANG Y, AN D, XU H, et al. On the symplectic superposition method for analytic free vibration solutions of right triangular plates[J]. *Archive of Applied Mechanics*, 2021, **91**(1): 187-203.
- [36] 杨雨诗, 安东琦, 倪卓凡, 等. 四角点支承四边自由矩形薄板屈曲问题的新解析解[J]. 计算力学学报, 2020, **37**(5): 517-523. (YANG Yushi, AN Dongqi, NI Zhuofan, et al. A new analytic solution to the buckling problem of rectangular thin plates with four corners point-supported and four edges free[J]. *Chinese Journal of Computational Mechanics*, 2020, **37**(5): 517-523. (in Chinese))
- [37] 李锐, 田宇, 郑新然, 等. 求解弹性地基上自由矩形中厚板弯曲问题的辛-叠加方法[J]. 应用数学和力学, 2018, **39**(8): 875-891. (LI Rui, TIAN Yu, ZHENG Xinran, et al. A symplectic superposition method for bending problems of free-edge rectangular thick plates resting on elastic foundations[J]. *Applied Mathematics and Mechanics*, 2018, **39**(8): 875-891. (in Chinese))
- [38] ZHANG D, ZHOU Y. A theoretical analysis of FGM thin plates based on physical neutral surface[J]. *Computational Materials Science*, 2008, **44**(2): 716-720.